

Non-Orthogonal Multiple Access for Diffusion-Based Molecular Communication Networks

Alexander Wietfeld
TU Munich, Germany
alexander.wietfeld@tum.de

Sebastian Schmidt
TU Munich, Germany
sebastian.a.schmidt@tum.de

Wolfgang Kellerer
TU Munich, Germany
wolfgang.kellerer@tum.de

ABSTRACT

This paper proposes a concept of non-orthogonal multiple access (NOMA) for diffusion-based molecular communication (DBMC) networks. The method relies on the difference in received signal levels for multiple access and uses successive interference cancellation. We analytically investigate the bit error probability (BEP) of a communication system using NOMA with two transmitters (TXs) and a central receiver. Initial results show that the BEP can be minimized by balancing a high received signal level from each TX with the separation in received signal level between the TXs. The identification of this trade-off is a first step towards the further analysis of NOMA for single-molecule-type multiple access in future DBMC networks.

KEYWORDS

molecular communication, non-orthogonal multiple access, NOMA

ACM Reference Format:

Alexander Wietfeld, Sebastian Schmidt, and Wolfgang Kellerer. 2023. Non-Orthogonal Multiple Access for Diffusion-Based Molecular Communication Networks. In *The 10th ACM International Conference on Nanoscale Computing and Communication (NANOCOM '23)*, September 20–22, 2023, Coventry, United Kingdom. ACM, New York, NY, USA, 2 pages. <https://doi.org/10.1145/3576781.3608741>

1 INTRODUCTION AND PHYSICAL SCENARIO

In future biomedical applications, molecular communication is expected to provide connectivity between multiple bio-nano sensors and a bio-cyber interface for distributed data gathering [5]. In order to distinguish between different data sources, this many-to-one scenario necessitates controlled multiple access (MA).

For diffusion-based molecular communication (DBMC), different MA schemes have been proposed and investigated, such as time-division MA (TDMA) [5] or molecular-division MA (MDMA) [1]. TDMA enables single-molecule MA while MDMA allows for simultaneous transmission. However, both properties are desirable for low complexity and high capacity DBMC systems [3]. This work investigates non-orthogonal MA (NOMA) based on successive interference cancellation (SIC) [4] applied to DBMC networks. The proposed method provides single-molecule MA as well as simultaneous transmission. For an initial analysis of NOMA in DBMC

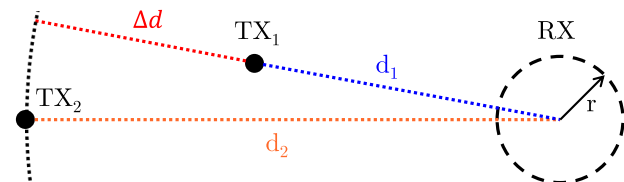


Figure 1: DBMC scenario with two point transmitters at distances d_1 and d_2 from a spherical receiver.

networks, the bit error probability (BEP) is derived for a simplified data gathering system, consisting of two TXs and one RX.

Figure 1 depicts the considered communication scenario with the TXs at distances d_1 and d_2 ($d_1 \leq d_2$) from the spherical RX with radius r . The TXs are modeled as point sources with instantaneous molecule release. All TXs emit the same type of molecule, which is affected by Brownian motion with diffusion coefficient D . The RX is assumed to be passive and the time-varying number of molecules within its bounds is the received signal, $n_{RX}(t)$.

For emission of a single molecule at $t = 0$, the probability of observing it at time t in a RX with volume V_{RX} at distance d is derived in [2] as

$$P(t, d) = \frac{V_{RX}}{(4\pi Dt)^{\frac{3}{2}}} \exp\left(-\frac{d^2}{4Dt}\right). \quad (1)$$

For pulse-like emission of N_{TX} molecules from a single TX, $n_{RX}(t)$ can be modeled as a Poisson-distributed random variable with mean $\lambda(t, d) = N_{TX}P(t, d)$ [6].

2 SYSTEM DESIGN AND BEP DERIVATION

To transmit information to the RX, both TX_i in Figure 1 send symbols $s_i \in \{0, 1\}$ with equal probability using pulse-based on-off-keying. We assume the symbol period to be sufficiently long such that inter-symbol interference (ISI) is negligible allowing us to focus on the interference between the TXs within a single symbol period.

For simultaneously transmitting TXs, $n_{RX}(t)$ is a sum of Poisson-distributed variables $n_{RX,i}(t)$ with means $s_i\lambda_i(t) = s_i\lambda(t, d_i)$. Thus, in the considered scenario $n_{RX}(t) \sim \mathcal{P}(s_1\lambda_1(t) + s_2\lambda_2(t))$. A SIC technique, similar to the one proposed for NOMA in [4], is used to separate the signals at the RX. In the first step, the message from TX_1 is detected from $n_{RX}(t)$ with $n_{RX,2}(t)$ considered as added interference. In the second step, the RX uses knowledge of the channel to subtract the estimated component of TX_1 from the received signal. The resulting signal is used for the detection of s_2 .

We assume perfect synchronization and distance estimation at the RX. Therefore, the RX can sample $n_{RX}(t)$ at the time of the expected peaks for each component $n_{RX,i}(t)$, given by $t_{p,i} = d_i^2/6D$.

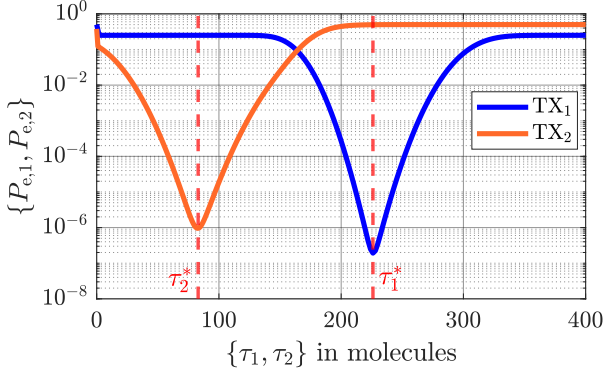


Figure 2: Bit error probabilities $P_{e,i}$ over the detection thresholds τ_i . For $P_{e,2}$, we assume $\tau_1 = \tau_1^*$ ($d_1 = 10 \mu\text{m}$, $d_2 = 12 \mu\text{m}$, $N_{\text{TX}} = 10^6$, $D = 10^{-9} \frac{\text{m}^2}{\text{s}}$, $r = 1 \mu\text{m}$).

The sample is decoded as $\hat{s}_i = 0$ if it is smaller than a threshold $\tau_i \in \mathbb{N}$ and as $\hat{s}_i = 1$ otherwise. The expected number of molecules from TX $_i$ at a sampling point is denoted as $s_i \lambda_{i,j} = s_i \lambda_i(t_{p,j})$.

For TX $_1$, the probability of the sample $n_{\text{RX}}(t_{p,1})$ being below τ_1 for any symbol combination is defined as

$$P_1^{s_1, s_2} = \mathbb{P}(n_{\text{RX}}(t_{p,1}) < \tau_1 | s_1, s_2) = \mathcal{P}_{\text{CDF}}(\tau_1 - 1; s_1 \lambda_{1,1} + s_2 \lambda_{2,1}), \quad (2)$$

where $\mathcal{P}_{\text{CDF}}(m; \lambda) = \sum_{k=0}^m \lambda^k \frac{e^{-\lambda}}{k!}$. By taking into account all symbol combinations, we can write the BEP of TX $_1$ as

$$P_{e,1} = \frac{1}{4} \left((1 - P_1^{0,0}) + (1 - P_1^{0,1}) + P_1^{1,0} + P_1^{1,1} \right). \quad (3)$$

For TX $_2$, SIC is incorporated by considering a sample, from which $\hat{s}_1 \lambda_{1,2}$, the estimated component from TX $_1$, has been subtracted. Consequently, the BEP for TX $_2$, $P_{e,2}$, depends on the previous detection step. Considering both possible cases for \hat{s}_1 , we define

$$P_2^{s_1, s_2} = \mathbb{P}(n_{\text{RX}}(t_{p,2}) - \hat{s}_1 \lambda_{1,2} < \tau_2 | s_1, s_2) = \mathbb{P}(\hat{s}_1=1 | s_1, s_2) \cdot \mathcal{P}_{\text{CDF}}(\tau_2 - 1 + \lambda_{1,2}; s_1 \lambda_{1,2} + s_2 \lambda_{2,2}) + \mathbb{P}(\hat{s}_1=0 | s_1, s_2) \cdot \mathcal{P}_{\text{CDF}}(\tau_2 - 1; s_1 \lambda_{1,2} + s_2 \lambda_{2,2}). \quad (4)$$

Here, $\mathbb{P}(\hat{s}_1 | s_1, s_2)$ represents the detection for TX $_1$ and can be calculated using Equation 2, e.g. $\mathbb{P}(\hat{s}_1=1 | s_1=1, s_2=1) = (1 - P_1^{1,1})$. Using Equation 4, $P_{e,2}$ can be written in analogy to Equation 3 and the BEP for the system can be defined as $P_{e,\text{sys}} = \frac{1}{2} (P_{e,1} + P_{e,2})$.

3 RESULTS AND CONCLUSION

Figure 2 depicts the value of $P_{e,i}$ over the respective τ_i for one choice of d_i . The results show that optimal threshold values τ_i^* , which minimize $P_{e,i}$ for both TXs can be found. $P_{e,2}$ depends on τ_1 , as shown in Equation 4. Therefore, we assume $\tau_1 = \tau_1^*$ before plotting $P_{e,2}$.

In Figure 3, the minimum achievable $P_{e,\text{sys}}$ found through threshold optimization via exhaustive search is shown on a heatmap as a function of d_1 and $\Delta d = d_2 - d_1$. The visible pattern is caused by two counteracting effects that can be analyzed in isolation. Firstly, the further either of the TXs is situated from the RX, the lower

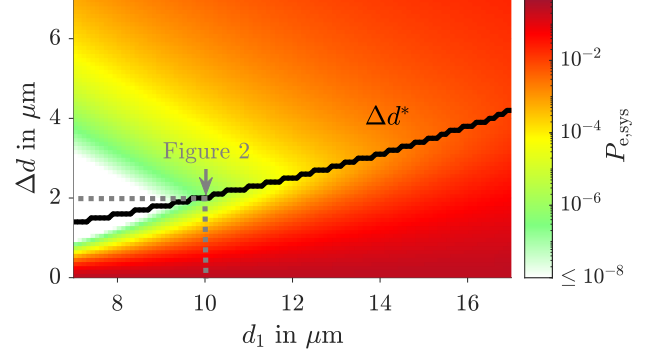


Figure 3: System bit error probability $P_{e,\text{sys}}$ with optimum thresholds for different values of d_1 and Δd . Optimum Δd^* , which minimizes $P_{e,\text{sys}}$ for given d_1 , is highlighted. Parameters used in Figure 2 are given as an example. ($N_{\text{TX}} = 10^6$, $D = 10^{-9} \frac{\text{m}^2}{\text{s}}$, $r = 1 \mu\text{m}$).

the received signal level from the TX, which causes a higher $P_{e,\text{sys}}$. Secondly, the greater Δd , the higher the separation between the two signal levels, which leads to a more effective SIC and therefore lower $P_{e,\text{sys}}$. For a given d_1 , there is always a Δd^* , which minimizes $P_{e,\text{sys}}$ representing the equilibrium point between the two effects.

The presented results suggest that signal-level-based NOMA with SIC has the potential to be a promising single-molecule MA method for DBMC systems. For a more realistic performance evaluation, we will extend the model to include the effects of ISI. Further, we plan for a generalization towards multiple TXs, performance comparisons with other MA schemes, investigation of adaptive TX signal levels, and simulation studies.

ACKNOWLEDGMENTS

Funded by the Federal Ministry of Education and Research of Germany in the program of ‘‘Souverän. Digital. Vernetzt.’’. Joint project 6G-life, project identification number: 16KISK002

REFERENCES

- [1] Xuan Chen, Miaowen Wen, Chan-Byoung Chae, Lie-Liang Yang, Fei Ji, and Kostromin Konstantin Igorevich. 2021. Resource Allocation for Multiuser Molecular Communication Systems Oriented to the Internet of Medical Things. *IEEE Internet of Things Journal* 8, 21 (Nov. 2021), 15939–15952.
- [2] Vahid Jamali, Arman Ahmadzadeh, Wayan Wicke, Adam Noel, and Robert Schober. 2019. Channel Modeling for Diffusive Molecular Communication—A Tutorial Review. *Proc. IEEE* 107, 7 (July 2019), 1256–1301.
- [3] Jong Woo Kwak, H. Birkan Yilmaz, Nariman Farsad, Chan-Byoung Chae, and Andrea J. Goldsmith. 2020. Two-Way Molecular Communications. *IEEE Transactions on Communications* 68, 6 (June 2020), 3550–3563.
- [4] Yuya Saito, Yoshihisa Kishiyama, Anass Benjebbour, Takehiro Nakamura, Anxin Li, and Kenichi Higuchi. 2013. Non-Orthogonal Multiple Access (NOMA) for Cellular Future Radio Access. In *2013 IEEE 77th Vehicular Technology Conference (VTC Spring)*. 1–5.
- [5] Ethungshan Shitiri and Ho-Shin Cho. 2021. A TDMA-Based Data Gathering Protocol for Molecular Communication via Diffusion-Based Nano-Sensor Networks. *IEEE Sensors Journal* 21, 17 (Sept. 2021), 19582–19595.
- [6] Jorge Torres Gómez, Ketki Pitke, Lukas Stratmann, and Falko Dressler. 2022. Age of Information in Molecular Communication Channels. *Digital Signal Processing* 124 (May 2022), 103108.